JACS
JOURNAL OF THE AMERICAN CHEMICAL SOCIETY
Article
pubs.acs.org/JACS

Single Molecular Resistive Switch Obtained via Sliding Multiple Anchoring Points and Varying Effective Wire Length

Manabu Kiguchi,*[,†] Tatsuhiko Ohto,[§,#] Shintaro Fujii,[†] Kazunori Sugiyasu,*[,∥] Shigeto Nakajima,[†] Masayuki Takeuchi,[∥] and Hisao Nakamura*[,§]

[†]Department of Chemistry, Graduate School of Science and Engineering, Tokyo Institute of Technology, 2-12-1 W4-10, Ookayama, Meguro-ku, Tokyo 152-8551, Japan

[§]Nanosystem Research Institute (NRI) "RICS," National Institute of Advanced Industrial Science and Technology (AIST), Central 2, Umezono 1-1-1, Tsukuba, Ibaraki 305-8568, Japan

[∥]Organic Materials Group, Polymer Materials Unit, National Institute for Materials Science, 1-2-1 Sengen, Tsukuba, Ibaraki 305-0047, Japan

Supporting Information

ABSTRACT: A single molecular resistive (conductance) switch via control of anchoring positions was examined by using a molecule consisting of more than two same anchors. For this purpose, we adopted the covered quaterthiophene (QT)-based molecular wire junction. The QT-based wire consisted of two thiophene ring anchors on each side; thus, shift of anchors was potentially possible without a change in the binding modes and distortion of the intramolecular structure. We observed three distinct conductance states by using scanning tunneling microscope-based break junction technique. A detailed analysis of the experimental data and first-principles calculations revealed that the mechanism of the resistive switch could be explained by standard length dependence (exponential decay) of conductance. Here, the length is the distance between the anchoring points, i.e., length of the bridged π-conjugated backbone. Most importantly, this effective tunneling length was variable via only controlling the anchoring positions in the same molecule. Furthermore, we experimentally showed the possibility of a dynamic switch of anchoring positions by mechanical control. The results suggested a distinct strategy to design functional devices via contact engineering.

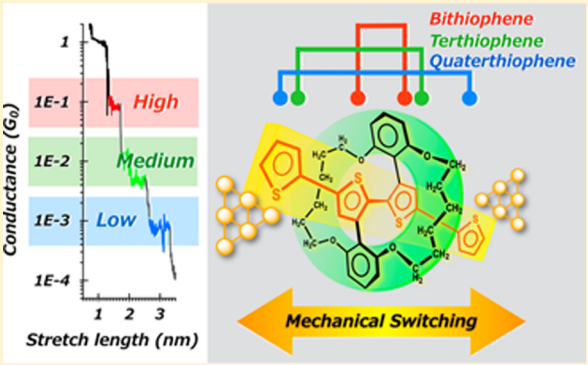

INTRODUCTION

Single molecular junctions have attracted attention owing to their potential applications as building blocks for realization of new functional electronic devices.[1,2] Because the fabrication of practical electronic devices requires wiring a single molecule into an electrical circuit, handling chemical structure of the contact point by the molecule and the electrode is quite important. Therefore, this contact engineering as well as molecular orbital (MO) engineering that focuses on designing electronic properties by tailoring conductor molecules has attracted great attention. The metal−molecule contact plays a decisive role in determining both the mechanical stability and electrical conductance. The most straightforward approach is searching either suitable atoms or chemical moieties as terminal anchors. Along this direction, various anchoring groups such as thiol (−SH), amine ($-NH_2$), isocyanide (−NC), cyanide (−CN), carboxylic acid (−COOH), selenol (−SeH), dimethyl phosphine ($-PMe_2$), and methyl sulfide (−SMe) have been investigated.[3−8] Recently, another type of anchoring—the direct binding of a π-conjugated molecule with the metal electrodes—has been proposed.[9] Because the contact was formed by metal−π interactions, it appears to be a promising technique for obtaining higher conductance than those obtained from the standard molecular junctions. Furthermore, the direct connection of a conductor molecule to electrodes provides many candidate anchoring positions in the carbon backbone; however, previous studies have not focused on this potential advantage.[9]

The possibility of tailoring functional devices such as rectifiers and transistors using molecular properties has been successfully demonstrated by MO engineering and highly advanced synthetic techniques.[10−13] The electronic coupling strength also affects electric transport properties,[12,14] and it strongly depends on the anchoring positions or chemical nature at the contact such as the binding mode. As a result, the topic of current research pertains to the control of device functions based on contact engineering. For example, the anchor moiety, which consists of two or more contact points, has been examined. Li et al. investigated the porphyrin molecular

Received: December 24, 2013
Published: March 13, 2014

   dx.doi.org/10.1021/ja413104g | J. Am. Chem. Soc. 2014, 136, 7327−7332

junction with four anchoring units, while Ie et al. developed the tripodal bipyridine anchoring units.[15,16] Although their main focus was the formation of mechanically robust contacts using multianchoring points, the results showed that a variety of contact configurations could also change transport properties. Hence, the dynamic control of metal-molecule contact could potentially lead to other routes to develop functional devices of the molecular resistive switching types.[17]

Quite recently, Venkatraman's group succeeded in investigating the switching functionality by controlling two different contact configurations within a single contact point, wherein the binding mode of the anchor to the Au electrode is changed.[18] In this study, we examined the possibility of dynamic control of anchoring sites and suggested single molecular resistive switching based on a different strategy, i.e., "switch of anchor in single molecule" without a change in either the binding modes or chemical structures of the contact. For this purpose, we investigated a quaterthiophene-based molecular wire (QT), which had two of the same anchors (i.e., thiophene rings, T1 and T2) at both the termini (Scheme 1a).

Scheme 1. (a) Chemical Structure and (b) Computer Generated Model of QT[a] and (c) Experimental Setup for the Conductance Measurement

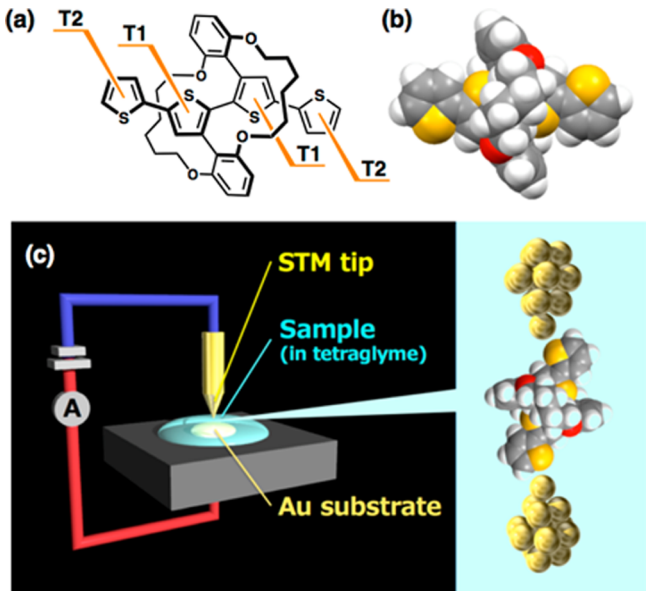

[a]QT molecular wire has more than two of the same anchors (i.e., T1 and T2) at both the termini.

These two termini were symmetrically separated by the "insulating" layer which prevented the intermolecular interactions among the QT molecules at the junction and enabled the measurement of single QT conductance. Because of this characteristic QT structure, the junction could be switched to T1-T1, T1-T2, and T2-T2 connections.

The measured conductance showed three distinct values: 0.05 G_0 (high-conductance state), 0.005 G_0 (medium-conductance state), and 0.0005 G_0 (low-conductance state), respectively. By estimating the distance between the contact points as well as tip-Au distance, we found that the resulting conductance was in line with the standard length dependence of off-resonant tunneling, i.e., exponential decay.[19] The stable structures of the contacts were determined from first-principles calculations. We found that the resistive switch was caused by varying the effective length of the conducting π-conjugate backbone via a change in the anchors; T1↔T2. The dynamic control of these three conductance states was also shown by mechanically controllable modulation.

RESULTS AND DISCUSSION

Conductance Measurements. Conductance measurements were performed using scanning tunneling microscopy-based break junction (STM-BJ) technique on an electrochemical STM (Pico-SPM, Molecular Imaging Co.) with a Nano Scope IIIa controller (Digital Instruments Co.) at room temperature and in ambient conditions. The details of the experimental design used in this study have previously been reported by a few of the present authors.[20] Briefly, the STM tip was made of an Au wire (diameter ≈ 0.25 mm, purity >99%). The Au(111) substrate was prepared by flame annealing followed by quenching. The concentrations of solutions of covered QT (Scheme 1c) in tetraethyleneglycol dimethyl ether (tetraglyme) were adjusted to 1 mM. The STM tip was repeatedly moved in and out of contact with the substrate in the solution at a rate of 15 nm/s at room temperature. The conductances were measured during the breaking process with an applied bias of 20 mV between the tip and the substrate. All the statistical data were obtained using a large number (>20 000) of individual conductance traces. The experiments were performed on three distinct samples.

Figure 1a shows typical conductance traces, wherein the Au contacts were broken in blank solution and solutions

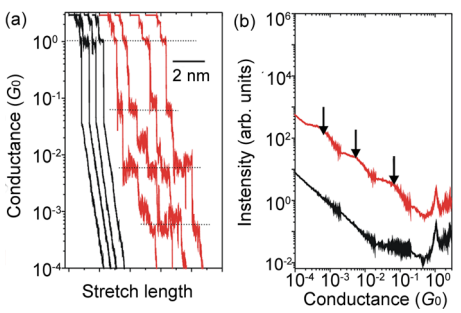

Figure 1. (a) Typical conductance traces of Au contacts in solution containing covered QT molecules (red) on a semilog scale. Black lines represent results in blank solution. (b) Conductance histograms constructed from 552 traces for covered QT, 1100 traces for blank shown on log−log plot (see Supporting Information for details). Conductance histogram for covered QT is scaled by 10.

containing covered QT molecules on a semilog scale. Most of the conductance traces showed a 1 G_0 plateau, indicating the formation of Au atomic contacts before the Au contacts were broken. In solutions containing covered QT molecules, additional conductance steps appeared in several conductance regimes below 1 G_0 (e.g., 0.05, 0.005, and 0.0005 G_0). The corresponding conductance histograms (Figure 1b) showed three distinct peaks, in addition to sharp peaks located at integer multiple of 1 G_0, which corresponded to Au atomic contacts. In blank solution, there were no features below 1 G_0 in the conductance histogram.

Figure 2a,c,e shows the typical conductance traces for covered QT on a linear scale. The conductance decreased in a stepwise fashion (dotted lines). The conductance value of the last plateau was around 0.05 G_0 (Figure 2a), 0.005 G_0 (Figure 2c), and 0.0005 G_0 (Figure 2e). In a few traces, we could see

dx.doi.org/10.1021/ja413104g | J. Am. Chem. Soc. 2014, 136, 7327−7332

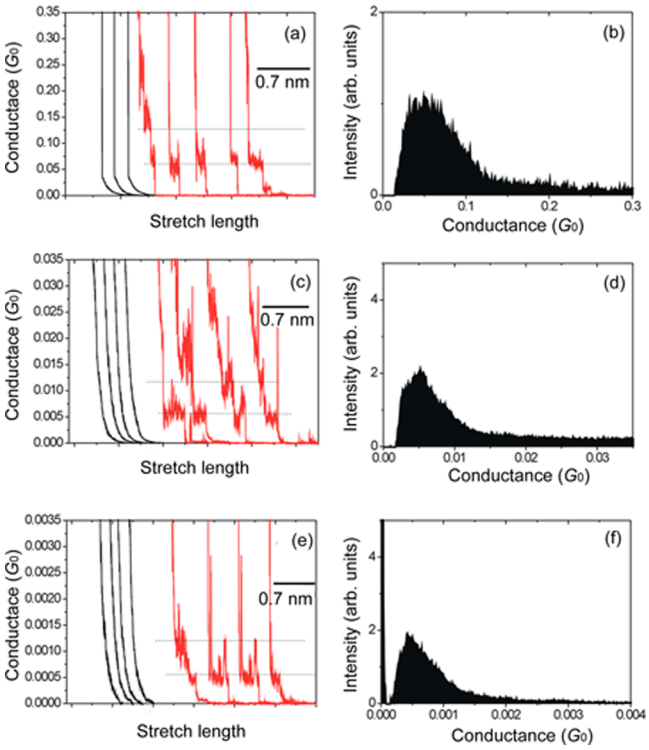

Figure 2. (a), (c), (e) Typical conductance traces of Au contacts in solution containing covered QT molecule at three different conductance regimes on a linear scale. Black line represents results obtained in blank solution. (b), (d), (f) Corresponding conductance histograms constructed from 522, 1255, and 979 traces at high-, medium-, and low-conductance regimes, respectively. Intensity was normalized with the number of conductance traces. Tunneling background was subtracted (see Supporting Information for details).

steps whose conductance values were twice that of the previous steps. Most of the steps showed either a positive or negative slope, which originated from a slight structural change in the molecular junction during the breaking of the junction. The corresponding conductance histograms (Figure 2b,d,f) showed distinctive features around 0.05 G_0 (Figure 2b), 0.005 G_0 (Figure 2d), and 0.0005 G_0 (Figure 2f). Neither plateau nor features were observed below 5×10^{-5} G_0 in the conductance traces and histograms. In the absence of the covered QT molecules, neither plateaus nor peaks were observed below 1 G_0 in both the conductance traces and histograms. On the basis of these experimental results, we concluded that the peak structures in the conductance histograms were because of the formation of single molecular junctions (Figure 2b,d,f), and the plateaux in the traces that appeared at an integer multiple of certain conductance corresponded to the multiple formations of the single molecular junctions (Figure 2a,c,e). The repeated conductance measurements revealed that the single covered QT molecular junction showed three distinct conductance values of 0.05 ± 0.03, 0.005 ± 0.003, and 0.0005 ± 0.0002 G_0. We called these as high-, medium-, and low-conductance states, respectively. Figure 3a,b shows the 2D conductance versus displacement histogram, which is analogous to the one found in previous reports (see Supporting Information).[21] We observed intense peaks around 0.05, 0.005, and 0.0005 G_0, which extended for distances of ca. 0.4, 0.7, and 1.2 nm, respectively, thereby indicating that single-molecule junctions were formed

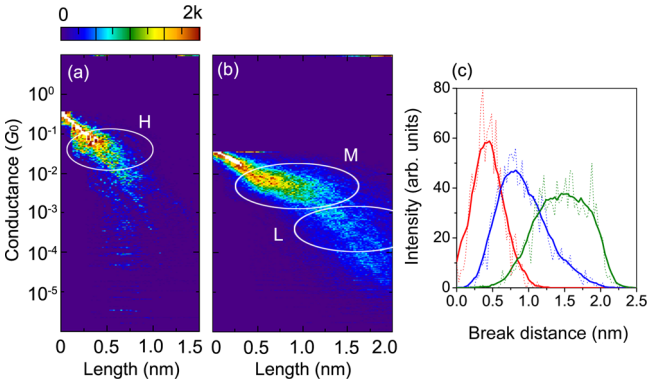

Figure 3. 2D conductance histograms constructed from (a) 522 and (b) 1255 traces for *H*, and *M* and *L* conductance regimes, respectively; white circles are eye-guides to highlight *H*-, *M*-, and *L*-conductance states. Bin sizes: ΔG = 50 bins per decade and ΔL = 0.02 nm. (c) Distribution of break distance of single-molecule junctions of covered QT. Red, green, and blue curves are results for *H*, *M*, and *L* conductance states, respectively. Distribution was obtained from 522 conductance traces without data selection.

reproducibly with this molecule and could be elongated over those distances.

In order to study the mechanism of conductance change, switch, we focused on the possible anchoring points in QT and effective length of the π-conjugated backbone bridging the anchors. The QT molecule had two thiophene rings on each side, which could bind to the Au electrode. Given the symmetrically sheathed structure, QT could connect the electrodes by three sets of left/right anchors, i.e., T1-T1, T1-T2, or T2-T2. To obtain information on the effective length of the molecular junctions, we analyzed break distances for the covered QT molecule junctions. The break distance analysis (Figure 3c) showed that the average gap distances were 0.33, 0.85, and 1.41 nm for the high (*H*), medium (*M*), and low (*L*) conductance states, respectively, for single covered QT molecular junctions (see Supporting Information for details).

The estimated gap distance of the single molecular junction was in reasonable agreement with the previous X-ray crystallographic study on the covered QT molecule,[22] wherein the S−S distances of T1-T1, T1-T2, and T2-T2 were found to be 0.44, 0.78, and 1.18 nm, respectively. This length could be considered as the length of π-conjugated backbone bridging the two terminal S atoms (Scheme 1). On the basis of the above effective length of H = 0.44 nm, M = 0.78 nm, and L = 1.18 nm, we analyzed the effective length dependence of single molecular conductance, i.e., $g \propto \exp(-\beta l)$, where β is decay constant and l is effective length and found that β was 0.46−0.75 Å^{-1}. A more detailed discussion on the β value and structure of the junction by first-principles calculations is included in the later section.

Dynamic Switch of Conductance Using Mechanical Control. Given the aforementioned results and the characteristic structure of QT, we envisaged that the switch of conductance was mechanically controllable. We repeated a mechanical elongation/compression by applying an ac voltage (triangle wave) to the piezo element that modulated the distance between the tip and the substrate. The resulting displacement amounted to 0.17 nm with a stretching speed of 5 nm/s. Figure 4 displays four examples of conductance switching of single covered QT molecule junctions. In the blank solution, the conductance regularly changed with the gap distance, wherein β was ca. 1 Å^{-1}. In the solution containing covered QT

dx.doi.org/10.1021/ja413104g | J. Am. Chem. Soc. 2014, 136, 7327−7332

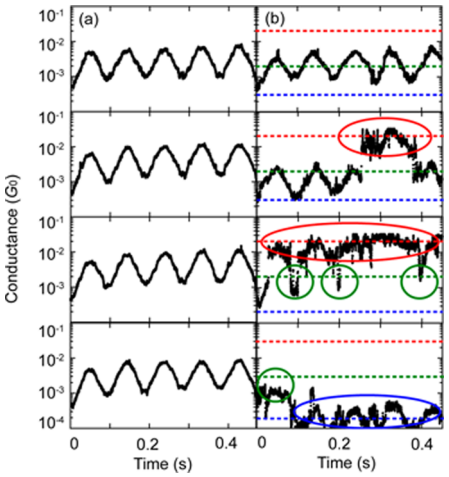

Figure 4. Examples of conductance traces measured during mechanical elongation/compression process at a bias voltage of 20 mV for solutions in the (a) absence and (b) presence of QT. Displacement is 0.17 nm with a stretching speed of 5 nm/s. Red, green, and blue lines and circles are guides for high-, medium-, and low-conductance states, respectively (red, green, and blue dotted lines indicate 0.02, 0.002, and 0.0003 G_0, respectively). These three conductance values correspond to mean values minus standard deviations of the single molecule conductance for *H*, *M*, and *L* states that obtained from statistical analysis of the conductance histograms (Figure 2). The difference in the preferable conductance values in Figure 2 and this figure can be ascribed to small variations in the preferential conformation of the Au−S point contact such as bond angle and length with and without ac distance modulation.

molecules, we observed the conductance switching among distinct conductance values that corresponded to high-, medium-, and low-conductance states of single QT molecule junctions (see red, green, and blue circles in Figure 4). In contrast with the regular conductance change in the blank solution, the conductance change was suppressed irrespective of the motion of the piezo element. The abrupt conductance change confirmed that the conductance switching indeed occurred via transitions between specific atomic configurations following a mechanically controllable modulation.

Theoretical Analysis. The analyses of conductance traces suggested a change in the distance between the end points of the molecule anchored onto the metal. To investigate the relationship between the atomistic structures of the contact and conductance, we performed first-principles calculations. Density functional theory (DFT)[23] was used for electronic structure calculations, wherein the Perdew−Burke−Ernzerhof (PBE) functional was employed for the exchange−correlation functional. The single-ζ polarized (SZP) basis set was used for Au, while a double-ζ polarized (DZP) level was adopted for the other atoms. Then, transport calculations were carried out using nonequilibrium Green's function method combined with DFT (NEGF-DFT).[24] The molecular junction consisted of a QT molecule and six monolayers plus the tip (apex) of Au for each side of the electrode, wherein the Au(111)-(6 × 8) structure was taken as the layers with the two-dimensional periodic boundary condition. We examined several conformations of the contact by changing the anchor moieties and positions in our first-principles calculations. Although the possible candidates for the contact are of three types, i.e., T1-T1, T1-T2, and T2-T2, the geometry of adsorption sites (binding modes) needs to be also considered. Figure 5 shows

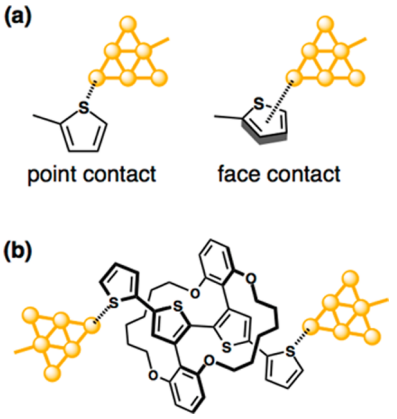

Figure 5. Schematic illustrations of QT-Au junctions used in calculations. (a) Two site types were considered and labeled as "point (P)" and "face (F)," respectively. Terminal S atom is anchoring to the tip of Au atom in the former type, while in the latter type, Au atom connects directly on the molecular plane of thiophene ring. (b) An example of the junction, wherein type is labeled as "T2(P)-T2(P)"; see also Figure 7.

the candidates for the contact geometries of the junction. On the basis of the chemical interaction of Au and thiophene ring, we assumed "point" and "face" sites, wherein the point site represented the bond between the terminal S and the tip Au atom, while the face site indicated the molecular plane of the thiophene ring contacts to the tip Au directly. Hence, the contact could be named by identifying the label of anchoring thiophene (T1, T2) moieties and the site type. For the sake of simplicity, we adopted the notation namely, T1(P)-T2(F) etc., which represented that the anchor T1 connected to Au by Au−S bond (i.e., point) and T2 used the face site. For each model contact, we determined the structure by optimizing the energy with relaxing molecular atoms and the tip−tip distance.

To compare the stability of the model junction, we evaluated the binding energy, E_{bind}, of the molecular contact as

$$E_{bind} = E_{mol} + E_{electrode} - E_{tot} \quad (1)$$

where E_{mol} and $E_{electrode}$ are the energy of the free molecule and electrode, respectively, and E_{tot} is the total energy of the unit cell. To calculate E_{bind}, we employed the counterpoise method to correct the basis set superposition error.[25] All of the calculated results are listed in the Table S1, and the summary is given in the lower panel of Figure 6 and plotted as a function of the tip−tip distance. We introduced the six conformations as the candidates of energy local minimum states. The series of the point contact structures had larger binding energies compared to that of the face (and face/point) contact. The calculated zero-bias conductance (*g*) for T1(P)-T1(P), T1(P)-T2(P), and T2(P)-T2(P) structures were 0.127, 0.029, and 0.015 G_0, respectively. The relative values of these three theoretical results agreed reasonably with those of the measured values though the absolute value of each conductance was overestimated owing to a well-known DFT error.[26] By analyzing the mechanical stability (binding energies) and relative conductance values, the three experimental conductance data can be assigned to the point-contact structures. Furthermore, we calculated the potential energy curve along the elongation coordinate (Au tip−tip distance) and found that the above three (P)-(P) type conformations were local minimum, while the other three structures, (P)-(F) and (F)-

dx.doi.org/10.1021/ja413104g | J. Am. Chem. Soc. 2014, 136, 7327−7332

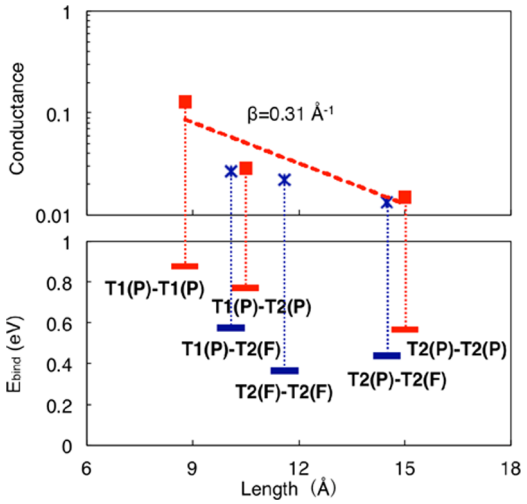

Figure 6. Conductance (upper panel) and binding energy (lower panel) of Au-QT-Au model junctions. Data are collocated as a function of distance of anchoring points. Data of point contact series (red square) are fitted using an exponential function. Dotted lines are only used as eye guides.

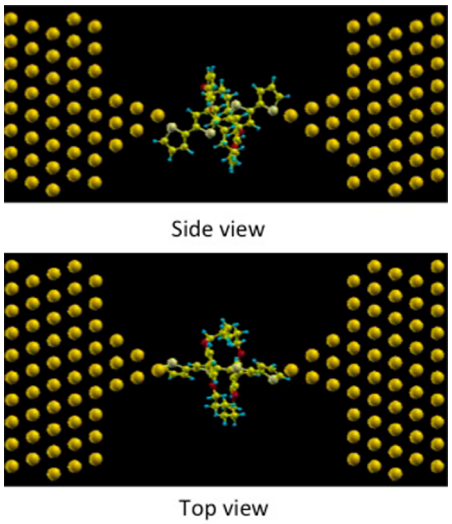

Figure 7. The view of optimized structure of T2(P)-T2(P) junction.

(F) types, were quasi-stable states (see Figure S6). Hence, we concluded that the suggested assignment is valid.

Because the T1-T1, T1-T2, and T2-T2 contacts consisted of two, three, and four thiophene rings as the backbone of the bridge between the anchors, respectively, it was equivalent to the increasing length of the carbon backbone of the junction, i.e., effective molecular wire length from bithiophene, terthiophene up to quaterthiophene. This supposition is justified by the calculation of electron pathway (local current vectors on each atomic site).[26] The details of calculations and results are presented in Figure S5. Thus, the length dependence of conductance, i.e., $g \propto \exp(-\beta l)$ was expected[19] at (P)-(P) type adsorption sites. As shown in Figure 6, we found a clear length dependence when the length was taken as the above effective molecular wire length (more strictly, number of thiophene rings between the anchor sites as the backbone). The theoretical value of β was 0.31 $Å^{-1}$, which was a typical order of magnitude for organic molecular wires. We also evaluated β by using the distance between the terminal S atoms; however, the value was only slightly larger than 0.31 $Å^{-1}$. By taking the band gap error of DFT into account, the theoretical β value agreed reasonably well with the experimental value, which was $0.46 \leq \beta$.[27]

We also calculated the conductance of the face contact models as references; however, the junctions were less stable than that of the point contact conformations. To discuss the effect of the anchoring type (point and face) to electronic coupling, we showed the top and side views of the T2(P)-T2(P) model as an example in Figure 7. The Au−S−C−C dihedral angle of the T2-T2 structure was 127°, which indicated that the electronic coupling of Au−S was formed by the mixing of the lone pair orbital of S and partial π-orbital of the thiophene ring. Therefore, a change in the adsorption site (binding mode) from face to point did not induce an order of magnitude reduction in the conductance, i.e., we could eliminate the possibility of the resistive switch by transitioning from/to point to/from face in the same anchor thiophene. A significant change in the conductance by conformational change from point to face contacts would be possible when the orientation of Au−S bond in the point contact structure is almost perpendicular to the π-orbital, i.e., electronic π contact is only possible by face contact structure analogous to the pyridine ring.[28] From these theoretical results, the observed varied (three) conductance values did not relate to the change in the chemical structures (binding modes). The mechanism of resistive switch of QT was essentially the standard length dependence of conductance; however, this length was modulated by the changing anchor positions.

CONCLUSION

We investigated the single molecular resistive switch of a partially covered QT molecular junction by means of STM break junction technique and first-principles calculations. The single molecular junction showed three distinct conductance states with values of 0.05 G_0 (high), 0.005 G_0 (medium), and 0.0005 G_0 (low). The distances between the Au electrodes in the molecular junctions were estimated to be 0.3 nm for high, 0.9 nm for medium, and 1.4 nm for low conductance states, respectively. The comparison between the experimental and theoretical analysis results revealed that the terminal S in the thiophene ring was bound to the tip Au atom and that the anchoring point shifted one by one in the QT moiety. The conductance changed upon varying the effective tunneling length in the molecular conductor owing to the shift in anchoring points and showed standard length dependence (exponential decay). Finally, we demonstrated that the contact configuration could be controlled by mechanical stretching of the junction. The synthesis of molecular materials containing equivalent multi-anchor moieties coupled with the dynamic control of anchor points using direct metal-molecule connection could be helpful in developing functional molecular devices of resistive switching types.

ASSOCIATED CONTENT

Supporting Information

Conductance measurements, and data analysis, and additional references. This material is available free of charge via the Internet at http://pubs.acs.org

dx.doi.org/10.1021/ja413104g | J. Am. Chem. Soc. 2014, 136, 7327−7332

AUTHOR INFORMATION

Corresponding Authors

kiguti@chem.titech.ac.jp
sugiyasu.kazunori@nims.go.jp
hs-nakamura@aist.go.jp

Present Address

[#]Osaka University Graduate School of Engineering Science Department of Materials Engineering Science Division of Materials Physics 1−3,Machikaneyama, Toyonaka, Osaka 560−8531, Japan.

Notes

The authors declare no competing financial interest.

ACKNOWLEDGMENTS

This work was financially supported by grants-in-aid for Scientific Research in Innovative Areas (no. 23111706), "Material Design through Computics: Complex Correlation and Non-equilibrium Dynamics" (no. 25104724); Electron, spin, and phonon transport through single molecule (no. 25104710)," and a grant-in-aid for Scientific Research (A) (no. 21340074) from the Ministry of Education, Culture, Sports, Science, and Technology (MEXT). H. N. also thanks the Grants-in-Aid for Scientific Research in Innovative Area-s,"Molecular Architectonics: Orchestration of Single Molecules for Novel Functions" (no. 20192461).

REFERENCES

(1) Cuevas, J. C.; Scheer, E. *Molecular Electronics: An Introduction to Theory and Experiment*; World Scientific Publishing Co. Pte. Ltd.: Singapore, 2010.
(2) Kiguchi, M.; Kaneko, S. *Phys. Chem. Chem. Phys.* **2013**, *15*, 2253.
(3) Chen, F.; Li, X.; Hihath, J.; Huang, Z.; Tao, N. J. *J. Am. Chem. Soc.* **2006**, *128*, 15874.
(4) Mishchenko, A.; Zotti, L. A.; Vonlanthen, D.; Bürkle, M.; Pauly, F.; Cuevas, J. C.; Mayor, M.; Wandlowski, T. *J. Am. Chem. Soc.* **2011**, *133*, 184.
(5) Haiss, W.; Wang, C.; Grace, I.; Batsanov, A. S.; Schiffrin, D. J.; Higgins, S. J.; Bryce, M. R.; Lambert, C. J.; Nichols, R. J. *Nat. Mat.* **2006**, *5*, 995.
(6) Mayor, M.; Weber, H. B.; Reichert, J.; Elbing, M.; von Hanisch, C.; Beckmann, D.; Fischer, M. *Angew. Chem., Int. Ed.* **2003**, *42*, 5834.
(7) Venkataraman, L.; Klare, J. E.; Tam, I. W.; Nuckolls, C.; Hybertsen, M. S.; Steigerwald, M. *Nano Lett.* **2006**, *6*, 458.
(8) Seminario, J. M.; De La Cruz, C. E.; Derosa, P. A. *J. Am. Chem. Soc.* **2001**, *123*, 5616.
(9) Kiguchi, M.; Tal, O.; Wohlthat, S.; Pauly, F.; Krieger, M.; Djukic, D.; Cuevas, J. C.; van Ruitenbeek, J. M. *Phys. Rev. Lett.* **2008**, *101*, 046801.
(10) Song, H.; Kim, Y.; Jang, Y. H.; Jeong, H.; Reed, M. A.; Lee, T. *Nature* **2009**, *462*, 1039.
(11) Dez-Perez, I.; Hihath, J.; Lee, Y.; Yu, L.; Adamska, L.; Kozhushner, M. A.; Oleynik, I. I.; Tao, N. *Nat. Chem.* **2009**, *1*, 635.
(12) Nakamura, H.; Asai, Y.; Hihath, J.; Bruot, C.; Tao, N. *J. Phys. Chem. C.* **2011**, *115*, 19931.
(13) Nakamura, H.; Ohto, T.; Ishida, T.; Asai, Y. *J. Am. Chem. Soc.* **2013**, *135*, 16545.
(14) Hines, T.; Díez-Pérez, I.; Nakamura, H.; Shimazaki, T.; Asai, Y.; Tao, N. *J. Am. Chem. Soc.* **2013**, *135*, 3319.
(15) Li, Z.; Borguet, E. *J. Am. Chem. Soc.* **2011**, *134*, 63.
(16) Ie, Y.; Hirose, T.; Nakamura, H.; Kiguchi, M.; Takagi, N.; Kawai, M.; Aso, Y. *J. Am. Chem. Soc.* **2011**, *133*, 3014.
(17) Ohto, T.; Runger, I.; Yamashita, K.; Nakamura, H.; Sanvito, S. *Phys. Rev. B* **2013**, *87*, 205439.
(18) Quek, S. Y.; Kamenetska, M.; Steigerwald, M. L.; Choi, H. J.; Louie, S. G.; Hybertsen, M. S.; Neaton, J. B.; Venkataraman, L. *Nat. Nanotechnol.* **2009**, *4*, 230.
(19) Asai, Y.; Fukuyama, H. *Phys. Rev. B* **2005**, *72*, 085431.
(20) Kiguchi, M.; Nakamura, H.; Takahashi, Y.; Takahashi, T.; Ohto, T. *J. Phys. Chem. C* **2010**, *114*, 22254.
(21) Perrin, M. L.; Prins, F.; Martin, C. A.; Shaikh, A. J.; Eelkema, R.; van Esch, J. H.; Briza, T.; Kaplanek, R.; Kral, V.; van Ruitenbeek, J. M.; J. van der Zant, H. S.; Dulic, D. *Angew. Chem., Int. Ed.* **2011**, *50*, 11223.
(22) Shomura, R.; Sugiyasu, K.; Yasuda, T.; Sato, A.; Takeuchi, M. *Macromolecules* **2012**, *45*, 3759.
(23) Soler, J. M.; Artacho, E.; Gale, J. D.; Garcia, A.; Junquera, J.; Ordejon, P. *J. Phys.: Condens. Matter* **2002**, *14*, 2745.
(24) Nakamura, H.; Yamashita, K. *J. Chem. Phys.* **2006**, *125*, 194106. Nakamura, H.; Yamashita, K.; Rocha, A. R.; Sanvito, S. *Phys. Rev. B* **2008**, *78*, 235420.
(25) Boys, S. F.; Bernardi, F. *Mol. Phys.* **1970**, *19*, 553.
(26) Nakamura, H. *J. Phys. Chem. C* **2010**, *114*, 12280.
(27) Toher, C.; Sanvito, S. *Phys. Rev. B* **2008**, *77*, 155402.
(28) Kamenetska, M.; Quek, S. Y.; Whalley, A. C.; Steigerwald, M. L.; Choi, H. J.; Louie, S. G.; Nuckolls, C.; Hybertsen, M. S.; Neaton, J. B.; Venkataraman, L. *J. Am. Chem. Soc.* **2010**, *132*, 6817.